Supporting Information

Methanogenic Biocathode Microbial Community Development and the Role of Bacteria

Christy M. Dykstra and Spyros G. Pavlostathis*

School of Civil and Environmental Engineering, Georgia Institute of Technology, 311 Ferst Drive, Atlanta, GA 30332-0512, USA

**Corresponding author*. Tel.: +404-894-9367; fax: +404-894-8266;

E-mail address: spyros.pavlostathis@ce.gatech.edu (S. G. Pavlostathis)

Journal:	Environmental Science & Technology
Date Prepared:	March 17, 2017
Text Sections:	S1 – S4
Tables:	S1 – S2
Figures:	S1 – S13
Pages:	20
References	

Text S1. DNA Analysis

Following extraction, all DNA was quantified using Nanodrop 3300 (Thermo Scientific, Wilmington, DE) and stored at -20°C until sequencing was performed. Amplified DNA was sequenced using the Illumina MiSeq platform (Research and Testing Laboratory, Lubbock, TX). Forward and reverse reads were merged with PEAR Illumina paired-end read merger and trimmed for quality. Clustering was performed at a 4% divergence using the USEARCH clustering algorithm and the UPARSE OTU selection algorithm was utilized to classify clusters into OTUs. Chimera checking of selected OTUs was performed with UCHIME software. Phylogenetic analysis was conducted by comparing sequences that had a relative abundance ≥1% with the closest 16S rRNA gene matches in GenBank (National Center for Biotechnology Information; Bethesda, MD). Using Mega 7.0 software, sequences were aligned with ClustalW and trimmed. A maximum likelihood phylogenetic tree was constructed using the Tamura-Nei model, 100 bootstrap replications and the Nearest-Neighbor-Interchange heuristic method.

Text S2. Enrichment of the Hydrogenotrophic Methanogenic (EHM) Suspended Growth Culture

The EHM culture was enriched for hydrogenotrophic methanogens by feeding a mixture of H_2 and CO_2. The headspace pressure decreased following each feeding (Figure S1A) because of gas dissolution into the medium and because hydrogenotrophic methanogenesis requires 5 moles of gas (4 H_2, 1 CO_2) to produce 1 mole of CH_4. Throughout each incubation cycle, the EHM culture pH remained stable at 6.8.

The culture headspace gas composition over the course of three representative 7-d feeding cycles is shown in Figure S1B. The mean daily H_2 and CO_2 removal rates were 69.1±6.9 mmol/d and 18.5±0.7 mmol/d (n = 3), respectively, representing a CO_2:H_2 removal ratio of 1:3.7, which is close to the theoretical stoichiometric ratio of 1:4 for hydrogenotrophic methanogenesis. The variation from the stoichiometric ratio may be due to differences in H_2 and CO_2 dissolution, microbial carbon storage and/or biomass production (168±5 mg/L TSS and 95±4 mg/L VSS at the end of a feeding cycle) (Dykstra and Pavlostathis, 2017).The culture actively produced CH_4 at a mean rate normalized to the total biomass (VSS) concentration over one feeding cycle equal to 1.96 mol CH_4/g VSS-d.

Text S3. Cyclic Voltammetry at Various Ionic Strengths

While all compared cyclic voltammograms (CVs) were conducted under similar conditions (e.g., scan rate, ionic strength, etc.), the effect of ionic strength on the shape and magnitude of the CV curve should be considered. In an abiotic system, ionic strength may affect the CV curve in two ways. First, an increase in ionic strength causes the diffuse layer of ions associated with the electrical double layer at the electrode surface to become compressed. As this layer becomes more compressed, redox-active molecules are able to approach the electrode surface more closely, enhancing electron transfer (Rieger, 2012). Thus, at a certain applied voltage, an increase in ionic strength is expected to increase current output. Second, an increase in conductivity, resulting from increased ionic strength, may reduce the ohmic potential drop, which is the required difference in potential to move ions in solution. This may result in the shifting of redox peaks (e.g., as ions migrate with a smaller ohmic potential drop, redox reactions may occur at lower applied voltages) (Britz, 1978).

To understand how ionic strength would affect the cyclic voltammetry of the system in this study, an abiotic BES was constructed as described in the Materials and Methods section of the main manuscript,

without inoculation of the anode and cathode. The anolyte and catholyte was 300 mM phosphate buffer medium (1.21 M ionic strength) and its ionic strength was increased stepwise from 1.21 M to 1.26, 1.31, 1.36 and 1.41 M by sequentially adding sodium chloride. CVs were conducted in triplicate. A representative CV for each ionic strength is plotted in Figure S4, which shows a trend of increasing current with increasing ionic strength, which follows expectations of double layer compression. Additionally, a more negative open circuit potential was observed at a higher ionic strength, which is consistent with a reduction in ohmic potential drop. Similar results were observed in a study that assessed the power generation of a microbial fuel cell in response to increasing ionic strength (Liu et al., 2005).

Text S4. Discussion of Proteobacteria in Suspended Growth and Cathode Biofilm Cultures.

α-Proteobacteria represented 2% and 4% of all *Proteobacteria* in the MM and MM-biocathode communities, respectively. In contrast, *α-Proteobacteria* increased from 1% to 26% of *Proteobacteria* between the EHM culture and EHM-biocathode. Within *α-Proteobacteria*, a phylotype similar to *Ochrobactrum* sp. was enriched on both the EHM- and MM-biocathodes. In the EHM and MM suspended growth cultures, this phylotype made up 17% and 77% of the *α-Proteobacteria*, respectively, but represented a respective 25% and 83% of EHM- and MM-biocathode *α-Proteobacteria*. *Ochrobactrum* species are known exoelectrogens capable of producing current from volatile fatty acids, sugars and alcohols (Logan, 2009; Liu et al., 1999; Matias et al., 2005).

β-Proteobacteria represented similar fractions of *Proteobacteria* in the MM and EHM cultures (18% and 14%, respectively) and each biocathode achieved similar enrichment to 47% and 35% of *Proteobacteria* in the MM- and EHM-biocathodes, respectively. Within *β-Proteobacteria*, a phylotype similar to *Achromobacter* sp. was enriched on both the EHM- and MM-biocathodes. In the EHM and MM suspended growth cultures, this phylotype made up 9% and 28% of the *β -Proteobacteria*, respectively, but represented a respective 39% and 55% of EHM- and MM-biocathode *β -Proteobacteria*. In fact, in the EHM-biocathode, the *Achromobacter* phylotype alone made up 6% of total Bacteria. *Achromobacter* enrichment on a biocathode with CO_2 as a sole external carbon source has previously been reported (Bond et al., 2002).

The *δ-Proteobacteria* composition differed between the MM and EHM suspended growth cultures (Table S2), with a greater relative abundance of phylotypes related to *Smithella* sp., *Desulfovibrionales* spp., and *Geobacter* sp. in the EHM culture than in the MM culture. *Smithella propionica* are syntrophic Bacteria that ferment propionate in association with methanogens that consume H_2 (McLennan et al., 2008). *Desulfovibrio* spp. are anaerobic Bacteria that are also capable of fermentation in association with methanogens during anaerobic digestion (Gölz et al., 2012). *Geobacter* species are well known exoelectrogens capable of utilizing organics such as acetate to produce current and CO_2 (Huang et al., 2015). *δ-Proteobacteria* represented a far smaller fraction of *Proteobacteria* in the MM- and EHM-biocathodes (19% and 0.5%, respectively) than in the MM and EHM inocula (64% and 14%, respectively). *δ-Proteobacteria* contains many sulfate- and iron-reducing species (Jeon et al., 2012), which require oxidized electron acceptors unlikely to be abundant near a highly-reduced cathode. In contrast, *Campylobacterales*, an order of ε-*Proteobacteria*, represented a moderately higher fraction of *Proteobacteria* in the MM- and EHM-biocathodes (5% and 11%, respectively) than in the MM and EHM inocula (2% and 7%, respectively). Many species of *Campylobacterales* possess surface polysaccharides that have been implicated in biofilm formation (Xu et al., 2011; Savelieva et al., 2004).

γ-*Proteobacteria* (64%) were the most abundant *Proteobacteria* in the EHM culture but made up only 12% of the MM culture *Proteobacteria* (Figure S11). Additionally, the γ-*Proteobacteria* composition was markedly different between the two cultures. In the EHM culture, 93% of γ-

Proteobacteria was made up of a phylotype similar to *Citrobacter freundii*. In both biocathodes, a phylotype similar to *Citrobacter* sp. dominated the *Enterobacteriaceae*, making up 97% and 99% of the *Enterobacteriaceae* in the EHM- and MM-biocathodes, respectively. This phylotype made up 3% of total Bacteria in the EHM-biocathode but only 0.5% of total Bacteria in the MM-biocathode. *Citrobacter* spp. have been shown to be exoelectrogens capable of utilizing a wide range of substrates and producing current in an MFC (Bouvet et al., 1995; Yong et al., 2011). In one study, a strain of *C. freundii* exhibited high electrochemical activity and was thought to transfer electrons through extracellular mediators (Bouvet et al., 1995), suggesting a potentially useful role in bioelectrochemical systems. *C. freundii* can ferment pyruvate, producing acetate, CO_2 and H_2, as well as small amounts of lactate, succinate and formate (Seviour et al., 2015; Price-Whelan et al., 2007). In the EHM culture, cell lysis products may have supplied fermentation substrates for *C. freundii*. However, it is not clear why *C. freundii* comprised such a large fraction (93%) of the *γ-Proteobacteria* in the EHM culture or what role it played in the microbial community.

The *γ-Proteobacteria* families represented in the MM culture were more diverse: *Enterobacteriaceae* (33%), *Vibrionaceae* (24%), *Xanthomonadaceae* (13%), *Pseudomonaceae* (12%) and unclassified (19%). In the MM culture, the most abundant family, *Enterobacteriaceae*, was dominated by a phylotype related to *Citrobacter* sp. (29% of *Enterobacteriaceae*), indicating a significant presence of *Citrobacter* phylotypes in both the MM and EHM cultures. Other families, such as the *Xanthomonadaceae*, *Pseudomonadaceae* and *Vibrionaceae* fell in relative abundance over the course of enrichment to 3%, 2% and below detection, respectively, in the EHM culture. Thus, enrichment conditions favored the growth of *Enterobacteriaceae*, in particular *Citrobacter*, over the growth of other types of *γ-Proteobacteria*.

The *γ-Proteobacteria* fraction of *Proteobacteria* increased between the MM inoculum (12%) and the MM-biocathode (20%), but decreased between the EHM inoculum (64%) and the EHM-biocathode (29%). The family composition of *γ-Proteobacteria* was also substantially different between the suspended growth cultures and the cathode biofilms. The family *Enterobacteriaceae* represented 69% of *γ-Proteobacteria* in the MM-biocathode but only 33% in the MM suspended growth culture. In contrast, *Enterobacteriaceae* represented 9% and 27% of the *γ-Proteobacteria* in the EHM and EHM-biocathode, respectively. Instead, *Pseudomonas* and *Xanthomonadales*, which represented only 2% and 3% of the *γ-Proteobacteria* in the EHM suspended growth culture, respectively, made up 54% and 19% in the EHM-biocathode, respectively.

Within the family of *γ-Proteobacteria*, the genus *Pseudomonas* was enriched on both biocathodes. *Pseudomonas* represented only 0.1% of the total Bacteria in the EHM suspended growth culture but made up 7% of all Bacteria in the EHM-biocathode biofilm. In the MM suspended growth culture, *Pseudomonas* made up only 0.03% of all Bacteria, which increased to 0.1% in the MM cathode biofilm. A previous study observed the enrichment of *Pseudomonas* on a cathode with CO_2 as a sole external carbon source (Bond et al., 2002). Within the genus, a phylotype similar to *Pseudomonas aeruginosa* represented 26% and 30% of *Pseudomonas* in the MM suspended growth culture and MM-biocathode biofilm, respectively, indicating not much change in *Pseudomonas* composition due to biofilm development. In contrast, the *P. aeruginosa* phylotype made up 100% of *Pseudomonas* in the EHM suspended growth culture and 70% of *Pseudomonas* in the EHM-biocathode. *P. aeruginosa* produces compounds, such as pyocyanin and phenazine, which are capable of acting as electron shuttles that can be utilized by other species for electron transfer in BESs (Logan, 2009; Pham et al., 2008). Indeed, phenazine has been shown to increase electron transfer in the anode of a MFC (Rabaey et al., 2005). Excretion of electron shuttles by *P. aeruginosa* appears to be associated with quorum sensing. In a study of a *P. aeruginosa* strain in which the *rhl* quorum sensing system was overexpressed, pyocyanin and phenazine-1-carboxylate were produced, with reduction potentials of -0.37 V and -0.48 V,

respectively (Leschine et al., 2006). Thus, excreted phenazines may act as mediators between a cathode surface poised at -0.80 V and the terminal electron acceptor, CO_2 ($E^{0'}$ = -0.24 V for CO_2/CH_4). Furthermore, another study showed *P. aeruginosa*-excreted pyocyanin concentrations were higher at more negative working electrode potentials (Veldkamp, 1960), although the tested potentials were not as negative as the cathode potential used in the present study (i.e., -0.8 V). Finally, phenazines are known to be produced when cell densities are high (Dollhopf et al., 2001), which is also consistent with microbial growth as a biofilm on the cathode. Thus, it is possible that the greater abundance of the *P. aeruginosa* phylotype in the EHM-biocathode contributed to the observed higher CH_4 production than in the MM-biocathode.

Table S1. Composition of *δ-Proteobacteria* in the MM and EHM suspended growth cultures

	MM Culture		EHM Culture	
Closest Matching Species	**Fraction of *δ-Proteobacteria***	**Fraction of Total Bacteria**	**Fraction of *δ-Proteobacteria***	**Fraction of Total Bacteria**
Unclassified *Syntrophobacterales*	58	0.8	19	0.2
Smithella sp.	26	0.4	49	0.6
Syntrophus spp.	7	0.1	7	0.09
Syntrophorhabdus sp.	6	0.08	3	0.04
Syntrophus buswelli	1	0.01	ND	ND
Geobacter sp.	2	0.02	4	0.05
Desulfovibrionales sp.	0.3	0.005	17	0.2
Desulfobulbus sp.	0.2	0.003	ND	ND
Sorangium cellulosum	ND[a]	ND	0.3	0.004
Desulfofaba sp.	ND	ND	0.2	0.003

[a] ND, not detected

Table S2. Closest GenBank Match and Relative Abundance of Identified Bacterial OTUs in the MM and EHM Suspended Growth and Biofilm Cultures

OTU	ID (%)	Closest GenBank Match	Relative Abundance[a] (%)			
			MM	MM-B	EHM	EHM-B
KU597466	90	NR_026182 *Actinomyces georgiae* strain DSM 6843	0	0	5	0
KU597440	90		2	2	0	0
KU597462	86	NR_074624 *Aminobacterium colombiense* strain DSM 12261	0	0	1	0
KU597439	87	NR_074383 *Anaerolinea thermophila* strain UNI-1	9	0	0	0
KU597471	88	FJ156092 *Arcobacter mytili* strain T234	0	0	1	1
KU597456	89		0	0	1	1
KU597452	99	DQ453797 *Bacterium* MB7-1	0	0	0	6
KU597464	99	AY949860 *Bacteroides* sp. strain Z4	0	0	8	0
KU597468	97		0	0	7	0
KU597425	98		0	9	0	0
KU597427	100		0	12	0	0
KU597451	99	LN564018 *Citrobacter amalonaticus* Y19	0	0	0	3
KU597463	86	NR_115465 *Cloacibacillus evryensis* strain 158	0	0	1	0
KU597438	88	L34418 *Clostridium herbivorans*	3	0	0	0
KU597467	90	NR_103938 *Clostridium pasteurianum* BC1 strain BC1	0	0	1	0
KU597435	88	NR_119085 *Clostridium polysaccharolyticum* strain DSM 1801	1	0	0	0
KU597433	99	NR_121725 *Eubacterium acidaminophilum* strain a1-2	1	0	0	0
KU597455	92	NR_118812 *Helicobacter cholecystus* strain Hkb-1	0	0	0	3
KU597437	100	NR_074986 *Lactobacillus crispatus* ST1 strain ST1	2	0	0	0
KU597460	93	NR_102952 *Mesotoga prima* strain MesG1.Ag.4.2	0	0	1	0
KU597461	95		0	0	52	0
KU597428	95		0	17	0	0
KU597429	94		5	3	0	0
KU597447	98	AF544628 *Mycobacterium frederiksbergense* isolate VM0503	0	0	0	5
KU597453	100	NR_074243 *Ochrobactrum anthropi* strain ATCC 49188	0	0	0	3
KU597436	79	NR_074586 *Pedobacter saltans* strain DSM 12145	3	0	0	0
KU597449	92	NR_025455 *Propionivibrio limicola* strain GolChi1	0	0	0	3
KU597457	92		0	0	0	3
KU597448	90	NR_044093 *Proteiniborus ethanoligenes* strain GW	0	0	0	1
KU597445	96	NR_043154 *Proteiniphilum acetatigenes* strain TB107	0	0	0	43
KU597434	94		0	1	0	0
KU597446	100	KR054983 *Pseudomonas aeruginosa* strain KAR21	0	0	0	5
KU597458	100	KR054989 *Pseudomonas grimontii* strain KAR27	0	0	0	1
KU597450	100	NR_115618 *Sphingopyxis terrae* strain IFO 15098	0	0	0	2
KU597465	77	NR_074795 *Spirochaeta thermophila* strain DSM 6578	0	0	2	0
KU597454	99	NR_074593 *Thiomonas intermedia* K12 strain K12	0	0	0	1
KU597469	88	NR_074169 *Treponema primitia* strain ZAS-2	0	0	5	0
KU597470	88		0	0	1	0
KU597426	89	AF023060 *Treponema* sp. I:K:T3	1	34	0	0
KU597430	99	NR_036793 *Trichococcus pasteurii* strain KoTa2	0	1	0	0
Other	NA	Minor species (< 1% relative abundance)	72	21	12	18

[a] Abbreviations: MM, mixed methanogenic suspended growth culture; EHM, enriched methanogenic suspended growth culture; MM-B, MM-inoculated biocathode; EHM-B, EHM-inoculated biocathode.

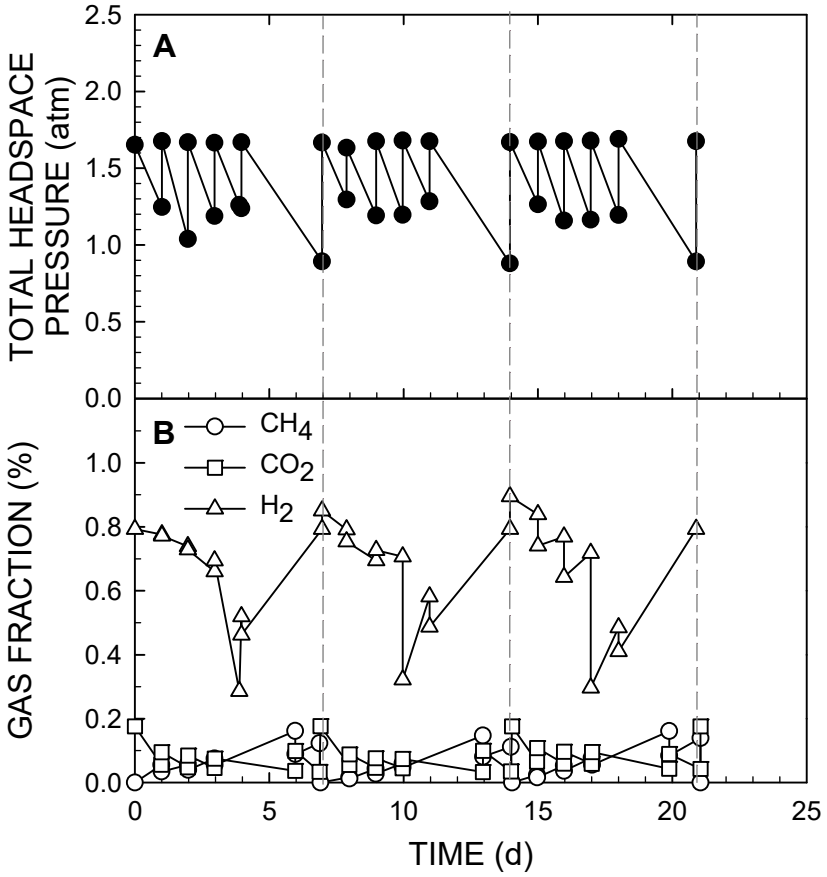

Figure S1. Headspace gas pressure (A) and gas composition (B) of the EHM suspended growth culture over three, representative feeding cycles. Dashed vertical lines indicate the wasting of a portion of the culture and replacement with fresh medium, accompanied by the complete flushing of the headspace with H_2/CO_2 (80:20 v:v). The increase in total headspace pressure on days other than those at the end of a 7-d feeding cycle (i.e., days not indicated by dashed vertical lines), was due to the addition of H_2/CO_2 without any gas release.

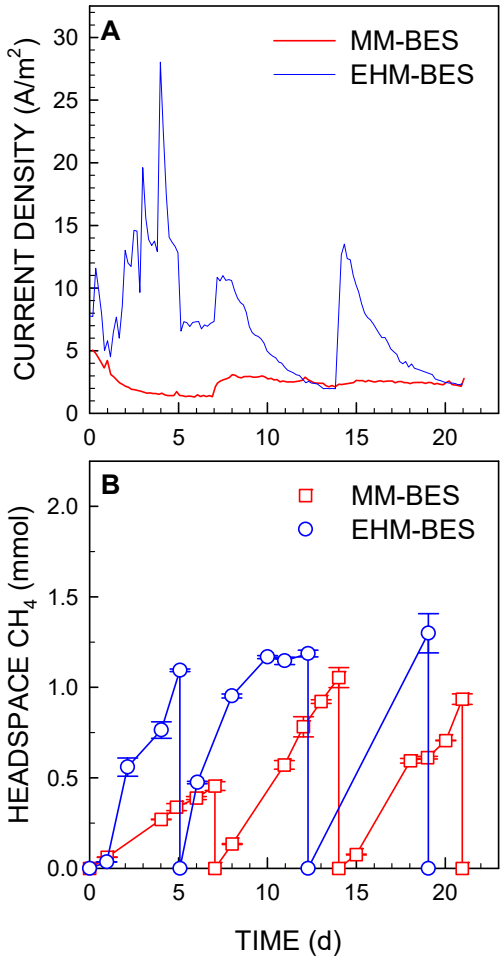

Figure S2. Time course of BES current density (A) and headspace methane (B) over the course of the first three feeding cycles for the MM-inoculated biocathode BES (MM-BES) and the EHM-inoculated biocathode BES (EHM-BES).

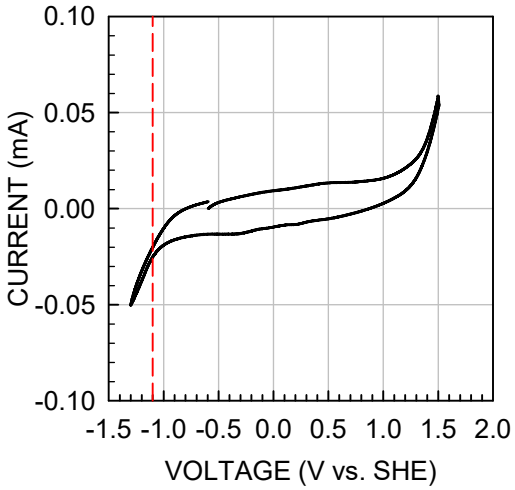

Figure S3. Cyclic voltammetry scan of inactive BES after the EHM-biocathode was maintained unfed in fresh catholyte and a N_2-filled headspace for 24 h. Scan conducted at a rate of 50 mV/s. Vertical broken line denotes an applied potential of -1.1 V at which H_2 evolution was noted.

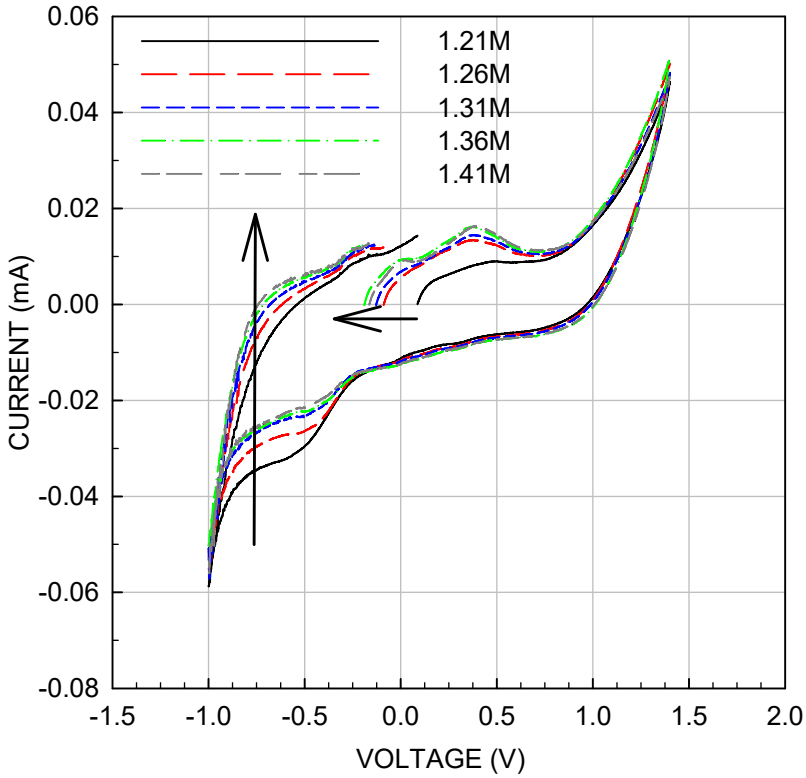

Figure S4. Cyclic voltammograms of an abiotic (i.e., uninoculated) BES with anolyte and catholyte at various ionic strengths (1.21, 1.26, 1.31, 1.36 and 1.41 M), starting at open circuit potential. Scans conducted at a scan rate of 50 mV/s. The vertical arrow shows how the CV curve shifts due to double layer compression, while the horizontal arrow shows how the open circuit potential shifts due to decreasing ohmic resistance.

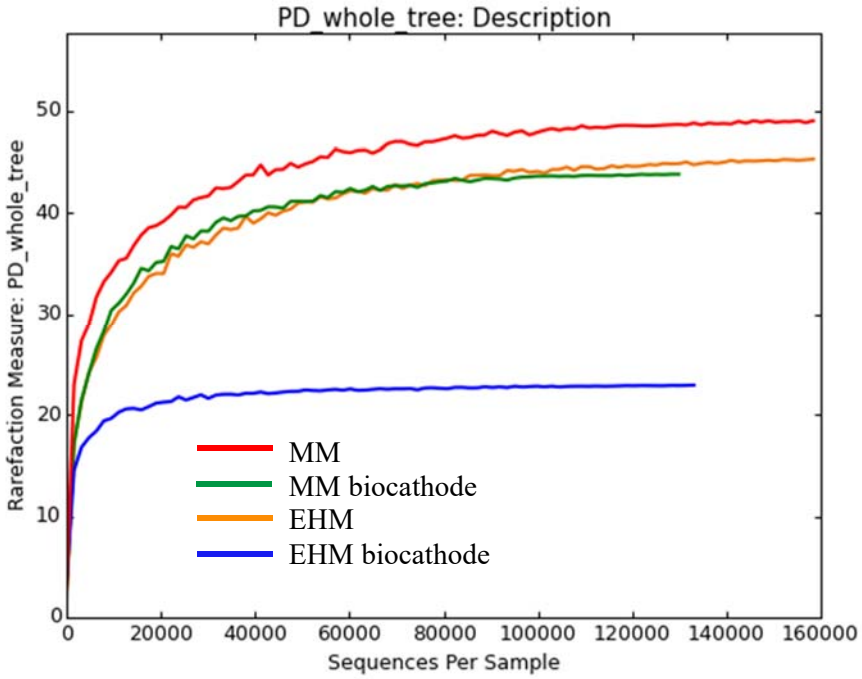

Figure S5. Rarefaction curves for the EHM culture, EHM biocathode, MM culture and MM biocathode. Lower and upper limits of rarefaction depths were 10 and 100, respectively, and the number of steps (i.e., rarefied OTU table sizes) was 100.

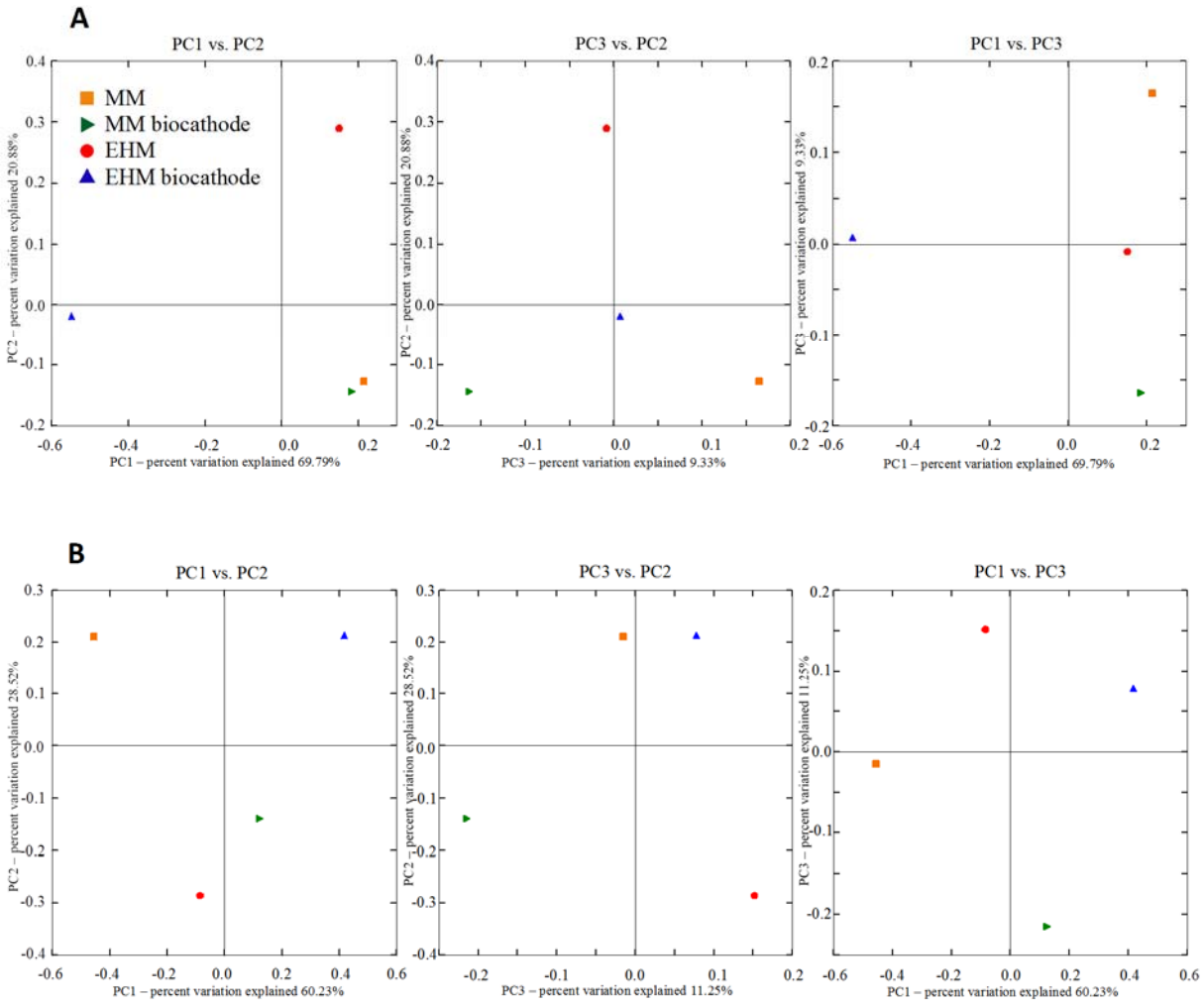

Figure S6. 2-D Principal Coordinate Analysis (PCA) plots for bacterial communities (A) and archaeal communities (B) of the MM suspended growth, MM biocathode, EHM suspended growth and EHM biocathode cultures.

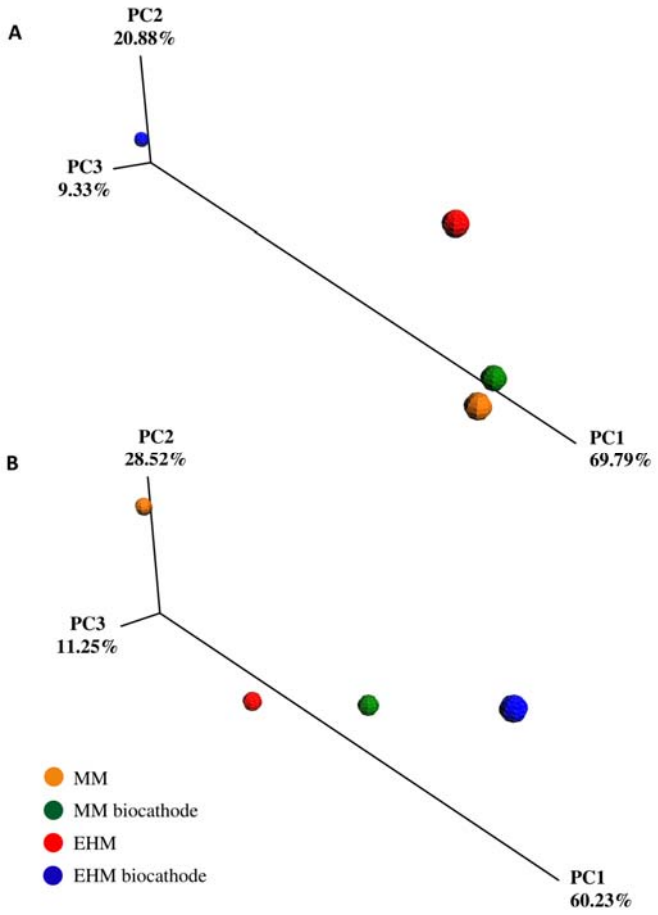

Figure S7. 3-D Principal Coordinate Analysis (PCA) plots for bacterial communities (A) and archaeal communities (B) of the MM suspended growth, MM biocathode, EHM suspended growth and EHM biocathode cultures. Axes are scaled to the percent variation explained by the principal coordinates.

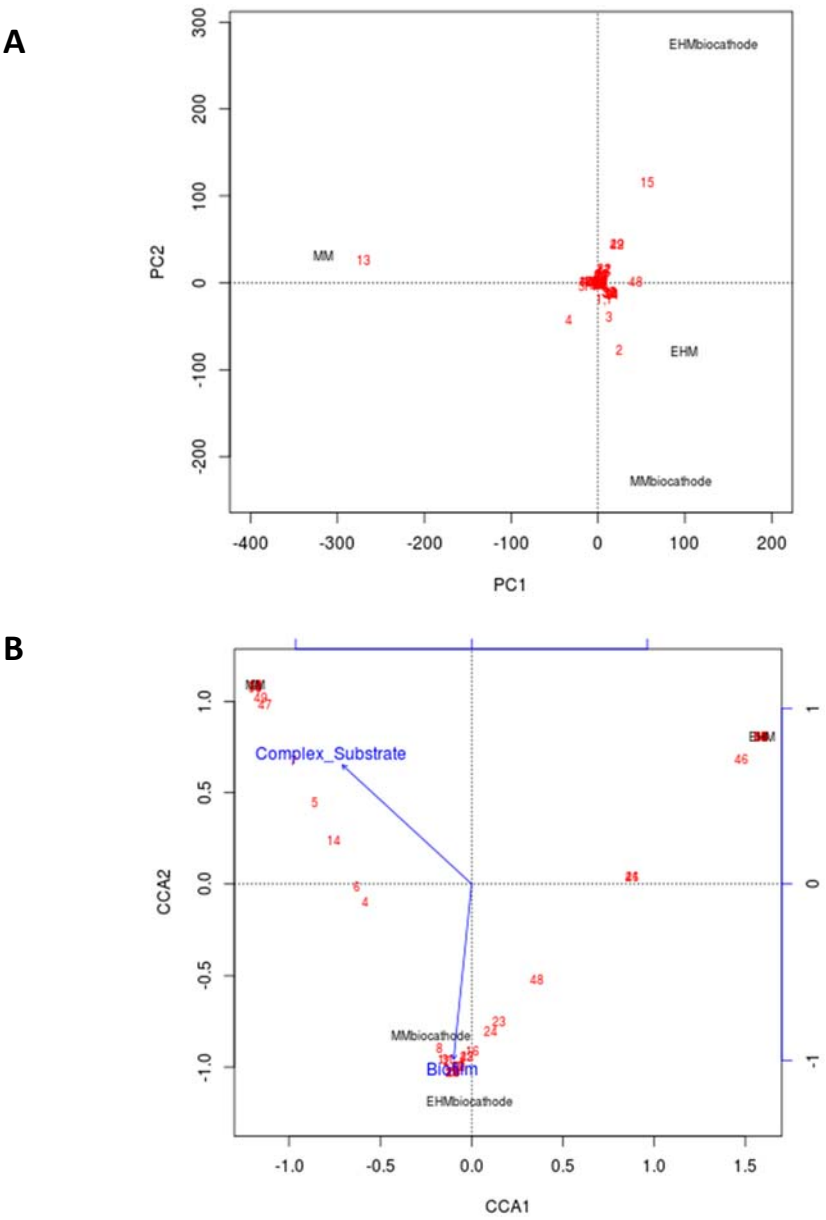

Figure S8. Redundancy analysis (A) and canonical correspondence analysis (B) plots to determine changes in OTU abundance attributed to biofilm development and higher buffer strength (MM Biocathode and EHM Biocathode), or higher temperature (35 vs. 22ºC) with a more complex (dextrin and peptone) substrate (MM culture). EHM was maintained with a lower buffer strength (100 vs. 300 mM) and a simple (CO_2/H_2) substrate.

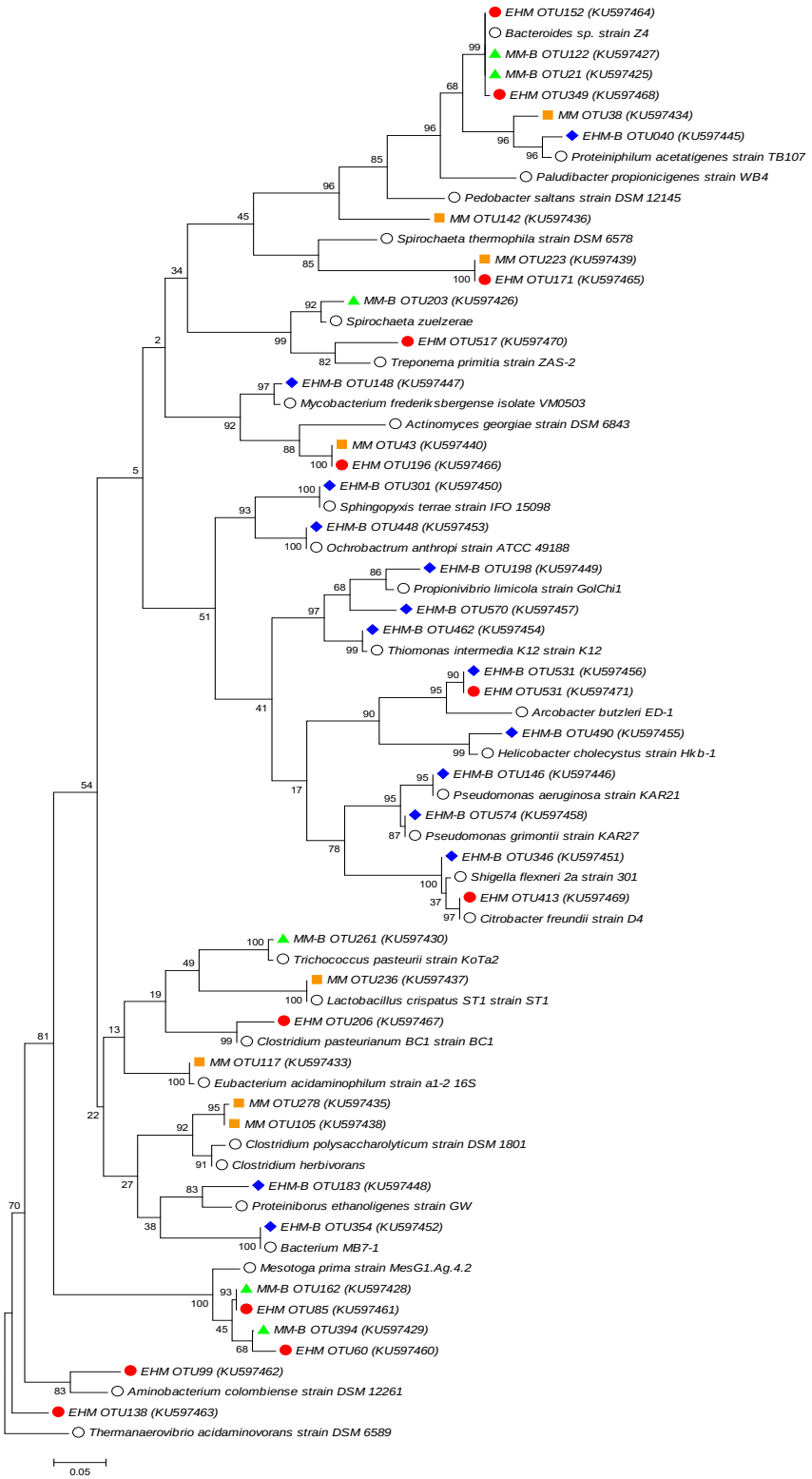

Figure S9. Phylogenetic tree showing the relationship of suspended growth cultures and BES biocathodes Bacteria OTUs (≥1% relative abundance) to their closest matched species in GenBank. Mixed methanogenic suspended growth culture (MM; orange square); MM-inoculated biocathode (MM-B; green triangle); Enriched hydrogenotrophic methanogenic suspended growth culture (EHM; red circle); EHM-inoculated biocathode (EHM-B; blue diamond).

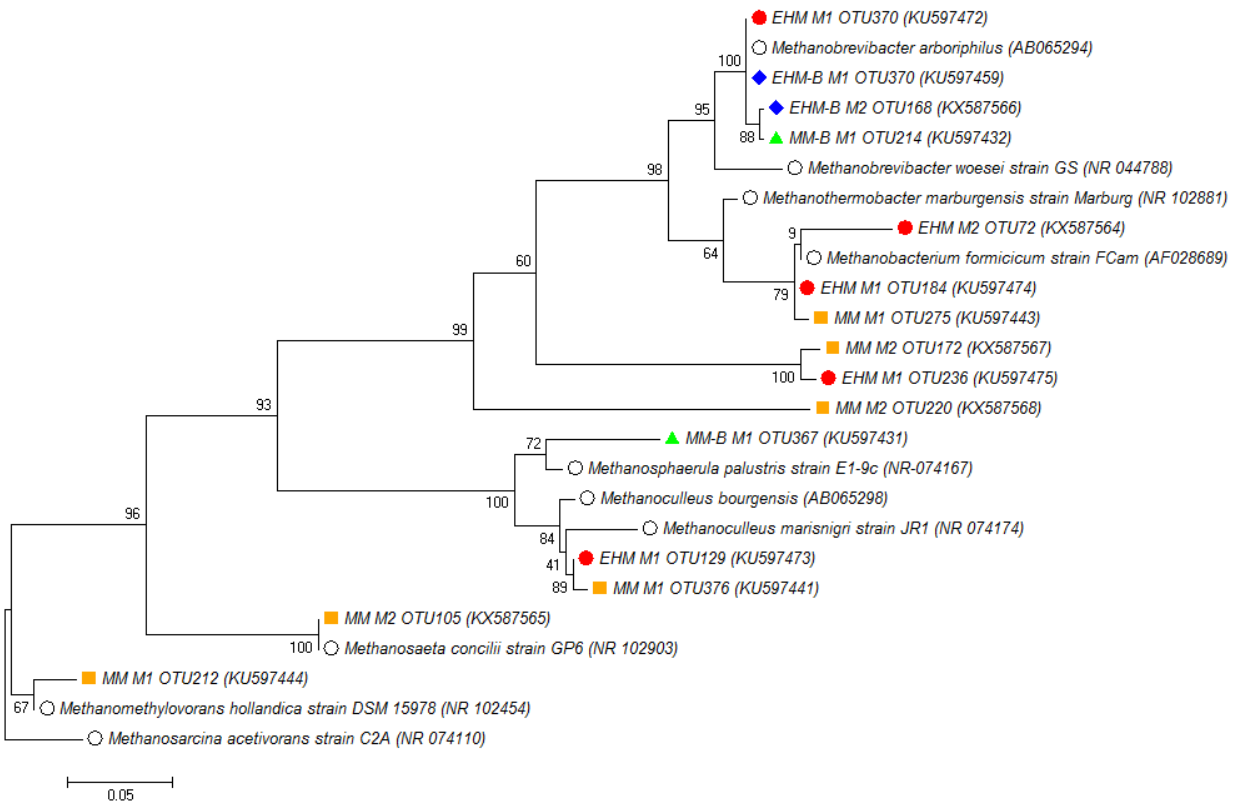

Figure S10. Phylogenetic tree showing the relationship of suspended growth cultures and BES biocathodes Archaea OTUs (≥1% relative abundance) to their closest matched species in GenBank. Mixed methanogenic suspended growth culture (MM; orange square); MM-inoculated biocathode (MM-B; green triangle); Enriched hydrogenotrophic methanogenic suspended growth culture (EHM; red circle); EHM-inoculated biocathode (EHM-B; blue diamond); DNA extraction method 1 (M1) and method 2 (M2)(See manuscript text).

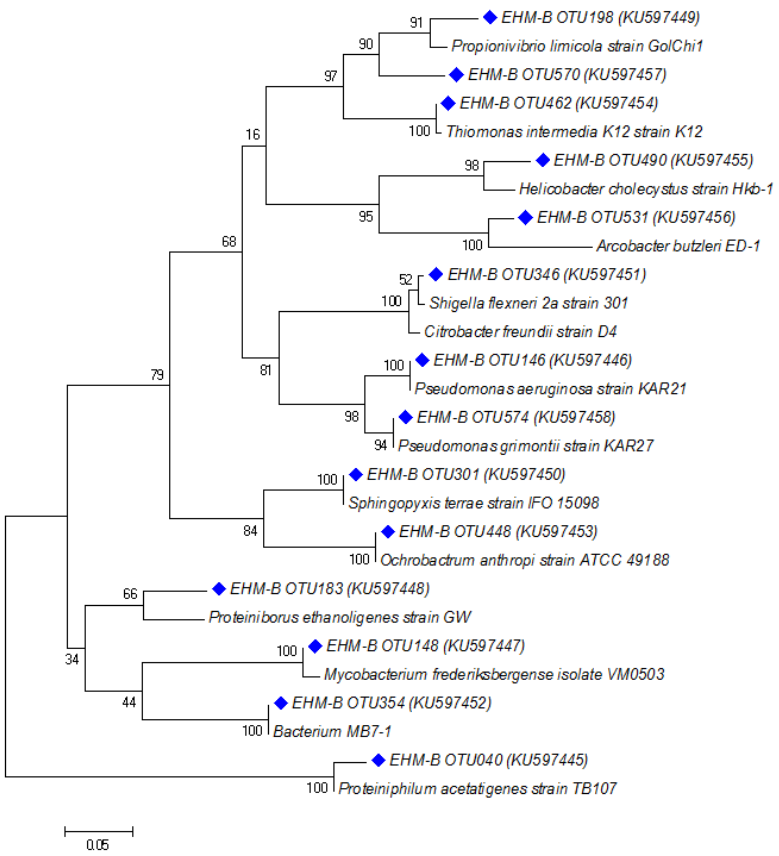

Figure S11. Phylogenetic tree showing the relationship of EHM-biocathode (EHM-B; blue diamond) Bacteria OTUs (≥1% relative abundance) to their closest matched species in GenBank.

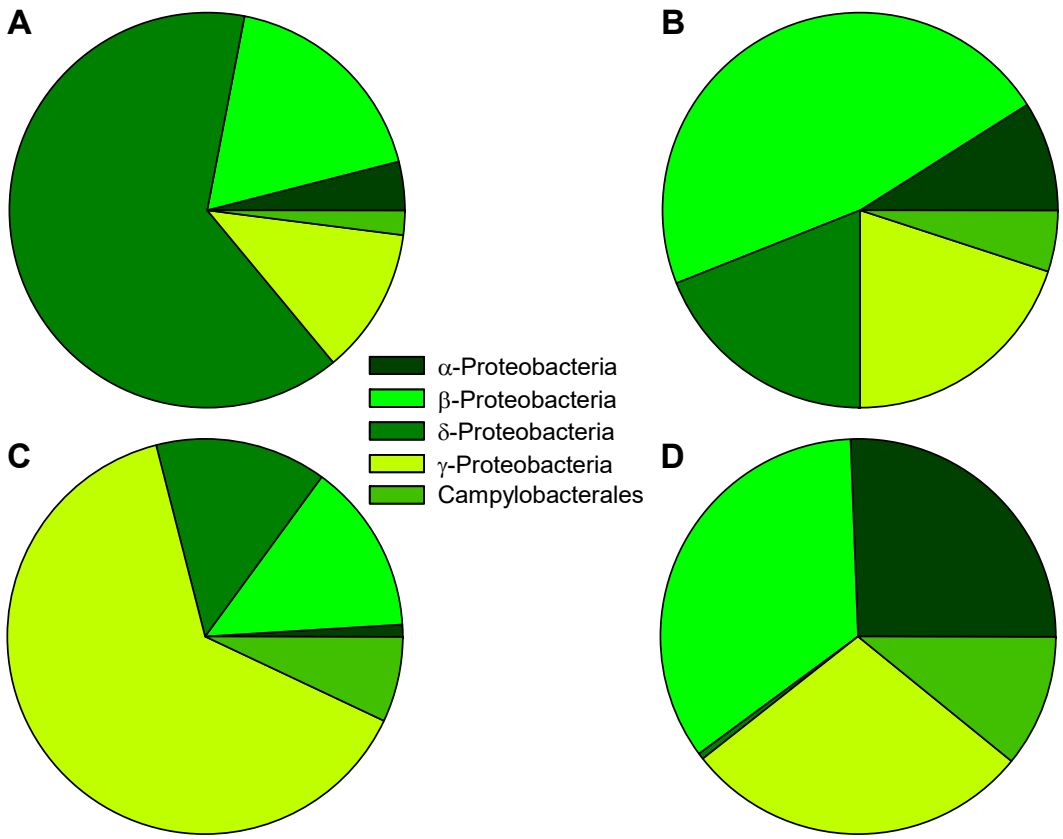

Figure S12. Relative abundance of classes within the phylum *Proteobacteria* for MM suspended growth culture (A), MM-inoculated biocathode BES (B), EHM suspended growth culture (C) and EHM-inoculated biocathode BES (D).

Culture	Relative Abundance of OTUs Related to Species of Various Categories (%)											
	CF	AAF	HP	HS	Ac	EE	HD	MP	BF	AB	CB	Unk
MM	22	15	10	1	1	4	0	0	2	6	0	75
MM-B	43	21	20	34	34	0	1	0	2	21	1	21
EHM	76	55	55	7	7	1	0	0	8	16	2	12
EHM-B	1	44	1	4	0	6	48	6	13	6	2	20

Figure S13. Relative abundance heatmap of OTUs most closely related to species classified as a carbohydrate fermenter (CF); amino acid fermenter (AAF); hydrogen producer (HP); hydrogen scavenger (HS); acetogen (Ac); exoelectrogen (EE); hydrocarbon degrader (HD); mediator producer (MP); implicated in biofilm formation (BF); found in anode biofilm (AB); found in cathode biofilm (CB); and unknown function (Unk). Mixed methanogenic suspended growth culture (MM); MM-inoculated biocathode (MM-B); Enriched hydrogenotrophic methanogenic suspended growth culture (EHM); EHM-inoculated biocathode (EHM-B). Note that most identified OTUs were related to species that belong to more than one class and, therefore, the row total for each culture exceeded 100%.

References

Bond, D. R.; Holmes, D. E.; Tender, L. M.; Lovley, D. R. Electrode-reducing microorganisms that harvest energy from marine sediments. *Science* 2002, 295 (5554), 483-485.

Bouvet, O. M. M.; Lenormand, P.; Ageron, E.; Grimont, P. A. D. Taxonomic diversity of anaerobic glycerol dissimilation in the Enterobacteriaceae. *Res. Microbiol*. 1995, 146 (4), 279-290.

Britz, D. iR elimination in electrochemical cells. *J. Electroanal. Chem. Interfacial Electrochem.* 1978, *88* (3) 309-352.

Dollhopf, S.; Hashsham, S.; Dazzo, F.; Hickey, R.; Criddle, C.; Tiedje, J. The impact of fermentative organisms on carbon flow in methanogenic systems under constant low-substrate conditions. *Appl. Microbiol. Biotechnol.* 2001, 56 (3-4), 531-538.

Dykstra, C. M.; Pavlostathis, S. G. Evaluation of gas and carbon transport in a methanogenic bioelectrochemical system (BES). *Biotechnol. Bioeng.* 2017, DOI 10.1002/bit.26230.

Gölz, G.; Sharbati, S.; Backert, S.; Alter, T. Quorum sensing dependent phenotypes and their molecular mechanisms in Campylobacterales. *Eur. J. Microbiol. Immunol*. 2012, 2 (1), 50-60.

Huang, J.; Zhu, N.; Cao, Y.; Peng, Y.; Wu, P.; Dong, W. Exoelectrogenic bacterium phylogenetically related to Citrobacter freundii, isolated from anodic biofilm of a microbial fuel cell. *Appl. Biochem. Biotechnol*. 2015, 175 (4), 1879-1891.

Jeon, B. Y.; Jung, I. L.; Park, D. H. Enrichment and isolation of CO2-fixing bacteria with electrochemical reducing power as a sole energy source. *J. Environ. Prot*. 2012, 3 (1), 55-60.

Leschine, S.; Paster, B.; Canale-Parola, E. Free-living saccharolytic Spirochetes: The genus Spirochaeta. In The Prokaryotes; Dworkin, M., Falkow, S., Rosenberg, E., Schleifer, K.-H., Stackebrandt, E., Eds.; Springer New York: New York 2006; pp 195-210.

Liu, H.; Cheng, S.; Logan, B. E. Power generation in fed-batch microbial fuel cells as a function of ionic strength, temperature, and reactor configuration. *Environ. Sci. Technol*. 2005, *39* (14) 5488-5493.

Liu, Y.; Balkwill, D. L.; Aldrich, H. C.; Drake, G. R.; Boone, D. R. Characterization of the anaerobic propionate-degrading syntrophs Smithella propionica gen. nov., sp. nov. and Syntrophobacter wolinii. *Int. J. Syst. Evol. Micr.* 1999, 49 (2), 545-556.

Logan, B. E. Exoelectrogenic bacteria that power microbial fuel cells. *Nat. Rev. Micro*. 2009, 7 (5), 375-381.

Matias, P. M.; Pereira, I. A. C.; Soares, C. M.; Carrondo, M. A. Sulphate respiration from hydrogen in Desulfovibrio bacteria: a structural biology overview. *Prog. Biophys. Mol. Biol.* 2005, 89 (3), 292-329.

McLennan, M. K.; Ringoir, D. D.; Frirdich, E.; Svensson, S. L.; Wells, D. H.; Jarrell, H.; Szymanski, C. M.; Gaynor, E. C. Campylobacter jejuni biofilms up-regulated in the absence of the stringent response utilize a calcofluor white-reactive polysaccharide. *J. Bacteriol.* 2008, 190 (3), 1097-1107.

Pham, T.; Boon, N.; Aelterman, P.; Clauwaert, P.; De Schamphelaire, L.; Vanhaecke, L.; De Maeyer, K.; Höfte, M.; Verstraete, W.; Rabaey, K. Metabolites produced by Pseudomonas sp. enable a gram-positive bacterium to achieve extracellular electron transfer. *Appl. Microbiol. Biotechnol.* 2008, 77 (5), 1119-1129.

Price-Whelan, A.; Dietrich, L. E. P.; Newman, D. K. Pyocyanin alters redox homeostasis and carbon flux through central metabolic pathways in Pseudomonas aeruginosa PA14. *J. Bacteriol.* 2007, 189 (17), 6372-6381.

Rabaey, K.; Boon, N.; Höfte, M.; Verstraete, W. Microbial phenazine production enhances electron transfer in biofuel cells. *Environ. Sci. Technol*. 2005, 39 (9), 3401-3408.
Rieger, P. H. *Electrochemistry.* 2012. Springer Netherlands.
Savelieva, O.; Kotova, I.; Roelofsen, W.; Stams, A. M.; Netrusov, A. Utilization of aminoaromatic acids by a methanogenic enrichment culture and by a novel Citrobacter freundii strain. *Arch. Microbiol.* 2004, 181 (2), 163-170.
Seviour, T.; Doyle, L. E.; Lauw, S. J. L.; Hinks, J.; Rice, S. A.; Nesatyy, V. J.; Webster, R. D.; Kjelleberg, S.; Marsili, E. Voltammetric profiling of redox-active metabolites expressed by Pseudomonas aeruginosa for diagnostic purposes. *Chem. Commun.* 2015, 51 (18), 3789-3792.
Veldkamp, H. Isolation and characteristics of Treponema zuelzerae nov. spec., an anaerobic, free-living spirochete. *Anton. Leeuw*. 1960, 26 (1), 103-125.
Xu, S.; Liu, H. New exoelectrogen Citrobacter sp. SX-1 isolated from a microbial fuel cell. *J. Appl. Microbiol.* 2011, 111 (5), 1108-1115.
Yong, Y.-C.; Yu, Y.-Y.; Li, C.-M.; Zhong, J.-J.; Song, H. Bioelectricity enhancement via overexpression of quorum sensing system in Pseudomonas aeruginosa-inoculated microbial fuel cells. *Biosens. Bioelectron.* 2011, 30 (1), 87-92.